

VLBI OBSERVATIONS AT 22.2 GIGAHERTZ OF THE RADIO SOURCE 0552+398 (DA 193)

ALAN L. FEY, STEVEN R. SPANGLER, AND ROBERT L. MUTEL

Department of Physics and Astronomy, University of Iowa

AND

JOHN M. BENSON

National Radio Astronomy Observatory¹

Received 1984 November 1; accepted 1985 February 13

ABSTRACT

We report 22.2 GHz observations of the quasar 0552+398 (DA 193). Our data are used to refine the source structure model and magnetic field estimate previously reported by Spangler and colleagues in 1983. We find the source to be more compact and the magnetic field to be weaker than indicated by the previous observations. We suggest that the object may be considered a highly compact, "naked core" object.

Subject headings: interferometry — quasars — radio sources: general

I. INTRODUCTION

The compact radio source 0552+398 (DA 193), which is identified with a high-redshift ($z = 2.365$) quasar, has an unusually peaked spectrum with a maximum in the range 5–6 GHz. Of 136 sources measured by Owen, Spangler, and Cotton (1980), 0552+398 had the steepest spectrum on the low-frequency side of maximum, with an optically thick spectral index close to the value of $5/2$ expected for a homogeneous synchrotron source. In addition, whereas most compact extragalactic radio sources show variability on time scales of months to years (Kellermann and Pauliny-Toth 1981), DA 193 has shown no evidence of significant variability over a period of about 6 yr.

In 1981 Very Long Baseline Interferometer (VLBI) observations at 6 and 2.8 cm were made of this source by Spangler, Mutel, and Benson (1983) (hereafter Paper I). Prior 2.8 cm observations of this source have been reported by Schilizzi and Shaver (1981). Because the source bears a striking resemblance to the theoretical ideal of a homogeneous synchrotron source, an accurate estimate of the magnetic field strength could be made. The magnetic field strength was then compared to the equipartition magnetic field estimate. The result was that the measured field was about a factor of 100 weaker than the equipartition value, i.e., that particle energy strongly dominated that of the magnetic field.

The purpose of this paper is to report 22 GHz VLBI observations which serve to refine the magnetic field estimates of Paper I. The present, high-frequency VLBI observations improve our magnetometry in two ways. First, the higher resolution afforded by 1.3 cm observations provides better estimates of the source structure than was possible from the 6 and 2.8 cm observations. Second, as will be seen in § III, the new observations strongly constrain the turnover frequencies of the source subcomponents. The net result of these observations is an improvement in our knowledge of both the source structure and magnetic field strength in DA 193.

II. OBSERVATIONS

a) Flux Density Measurements

The measurements of the integrated radio spectrum are from broad-band measurements made by Owen, Spangler, and Cotton (1980) and unpublished VLA observations. All of the flux density data are plotted in Figure 1a. The dashed curve represents a model fit to the spectrum, which is discussed below. The data, which were taken at epochs 1978.0, 1982.1, and 1984.3, are in quite good internal agreement. While observations at three epochs do not constitute a rigorous variability monitoring project, our data show no evidence for significant flux density variability in the period 1978.0–1984.3. We obviously cannot preclude the possibility that the source varied between the times of observation.

b) VLBI Observations

Observations were made at 1.3 cm (22.2 GHz) in 1983 February, using the United States VLBI Network and the 100 m telescope of the Max-Planck-Institut für Radioastronomie. The five-element interferometer consisted of antennas at Effelsburg, West Germany, Green Bank, W. Va., Westford, Mass., Socorro, N.M., and Owens Valley, Cal. The video tapes were correlated with the NRAO processor in Charlottesville, Va.

VLBI observations at a frequency of 22 GHz are somewhat challenging from a technical point of view, so a few words are in order regarding calibration procedures. The primary difficulty arises in visibility amplitude calibration, due to highly variable antenna gain, pointing errors, and atmospheric extinction due to water vapor.

Fortunately, for three of the stations (MPI, NRAO, and OVRO), source temperature measurements were logged on a regular basis throughout the observations. These source temperature measurements, which reflect the true antenna sensitivity including the aforementioned degradations, were used directly in the visibility calibration. For the single VLA antenna, we assumed a constant antenna sensitivity. The atmospheric extinction at the VLA site was measured during the observing session using a technique described in Spangler (1982). The resultant, directly measured, extinction coefficient was used to correct visibilities on baselines to the VLA. For the

¹ The National Radio Astronomy Observatory is operated by Associated Universities, Inc., under contract from the National Science Foundation.

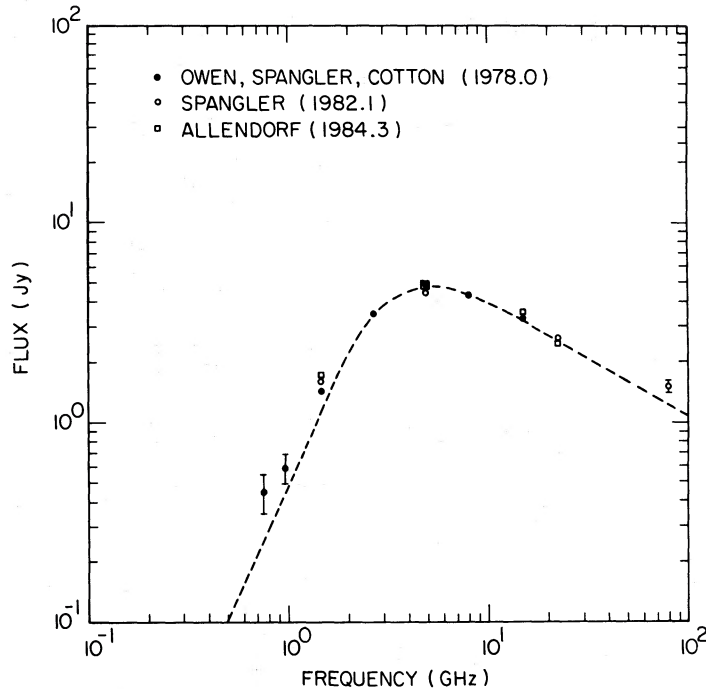


FIG. 1a.—Spectrum of 0552 + 398 in the frequency range 750 MHz to 90 GHz. Different symbols indicate measurements made in early 1978, 1982, and early 1984, respectively. The dashed curve represents a two-component model which is consistent with the VLBI observations. Data for epoch 1978.0 are from Owen, Spangler, and Cotton (1978); those for epoch 1982.1 are from the project described in Spangler and Cotton (1982); and data for epoch 1984.3 are from Allendorf (1985).

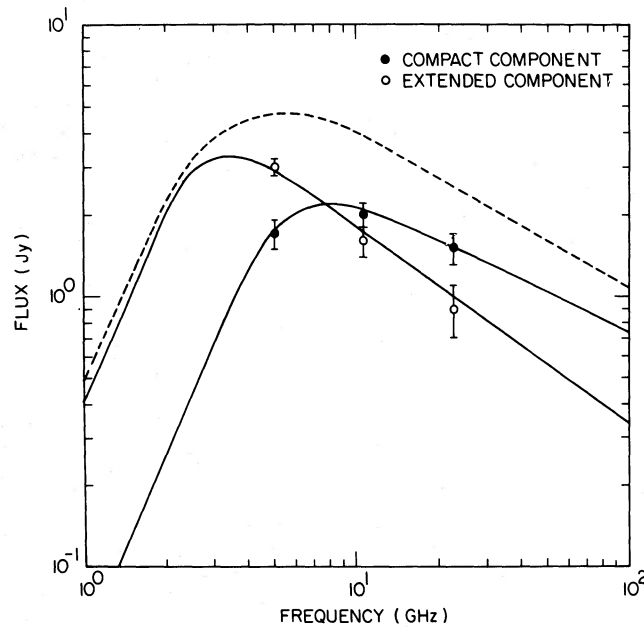


FIG. 1b.—Two-component model consistent with the VLBI observations. Different symbols indicate VLBI measurements for the compact and extended component, respectively. The dashed curve represents the sum of the component spectra. Measurements at 5 and 10.6 GHz are from Paper I.

Haystack antenna, we used a published curve of antenna sensitivity versus zenith angle. Extinction measurements were not possible, so a zenith extinction of 0.10 was assumed. Visibilities on baselines to Haystack were then corrected for zenith angle-dependent antenna gain and atmospheric extinction.

An indication of the integrity of our calibration is as follows. During the first iteration of hybrid mapping involving amplitude self-calibration (to be discussed below), the algorithm was

permitted to adjust each station gain by only a session-specific factor. The corrections were less than 10% for all stations, indicating that our initial calibration was satisfactorily accurate.

The calibrated data (correlated flux density and closure phase) were analyzed in three ways: (1) hybrid maps, (2) model fitting, and (3) study of plots of visibility versus projected baseline length.

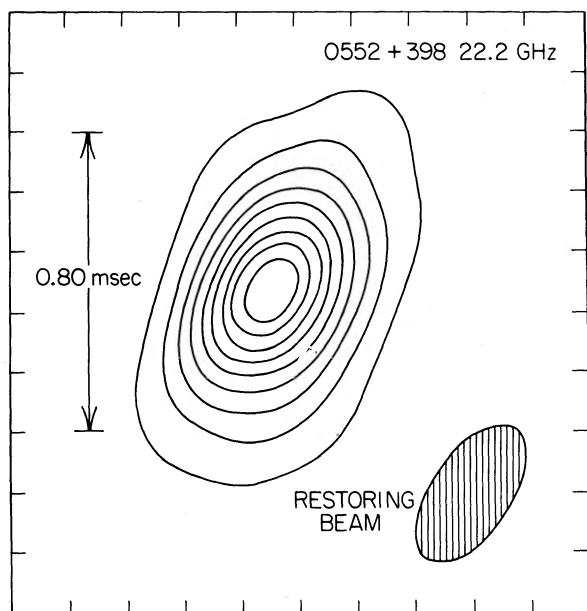


FIG. 2.—Hybrid map of 0552 + 398 at 1.3 cm. The contours are at 10, 20, 30, 40, 50, 60, 70, 80, and 90% of the peak intensity which is 1.068 Jy per beam. The restoring beam is 0.44×0.22 mas at position angle -37° . The rms noise in the residual map is 0.009 Jy per beam, with a maximum residual of 0.029 Jy per beam.

The hybrid map was made with three iterations of the algorithm developed by Readhead and Wilkinson (1978). The last two iterations employed amplitude self-calibration. A contour map is shown in Figure 2. It should be noted that the zero-spacing flux, i.e., the correlated flux on a baseline of zero length, does not equal the single dish flux of 2.83 Jy, measured during the observations with the Bonn telescope. However, the zero-spacing flux is within 15% of the single-dish flux, which may be considered acceptable for VLBI observations at this frequency, and the discrepancy may be assumed to be a calibration error.

As in the previous observations (Paper I), an attempt was made to fit a two-component elliptical Gaussian model to the data. The results of the model fitting are presented in Table 1. The quoted errors are estimates based on parameter ranges which gave equally good fits to the data in the least-squares model-fitting routine. The goodness of fit was determined mainly by the angular sizes and flux densities of the components. Because of the scatter in the closure phase data, an accurate determination of the separation of the two components was not possible. However, by constructing models with different separations and examining plots of these models,

TABLE 1

STRUCTURE OF 0552 + 398 AT 1.3 CENTIMETERS: TWO-COMPONENT GAUSSIAN MODEL

Parameter	Component 1	Component 2
Flux density (Jy)	1.5 ± 0.2	0.9 ± 0.2
Angular size (FWHM) (mas)	0.25 ± 0.03	0.63 ± 0.08
Axial ratio	0.77 ± 0.04	0.70 ± 0.17

NOTES.—Separation of components: ≤ 0.3 mas. Preferred position angle of line joining components: $\sim 180^\circ$. Angular size of source as a whole (for baseline lengths $\leq 2.0 \times 10^8$ wavelengths): θ (FWHM) = 0.35 ± 0.05 mas.

it was possible to set an upper limit to the separation of the two components. This analysis gave a component separation of ≤ 0.3 mas. We also computed the reduced χ^2 of the fit to amplitude and closure phase for the final two-component model. We then varied the separation and position angle of separation of the components and examined the behavior of χ^2 . The results of these “goodness-of-fit” tests confirmed that the separation of components is ≤ 0.3 mas.

It should be noted that a single Gaussian component does not provide a satisfactory fit to the data. Three arguments may be summoned to support this statement. First, the reduced χ^2 of the single component fit significantly exceeds that of the two-component model. Second, a single-component model was initially presented to the hybrid mapping algorithm, which produced a two-component map. Third, a comparison was made of the calibration-independent closure amplitudes with the single- and double-component models. The double-component model furnished a perceptibly superior fit to the data.

Finally, a plot of visibility amplitude versus projected baseline length, $(u^2 + v^2)^{1/2}$, shown in Figure 3 was studied. For baseline lengths shorter than about 2.0×10^8 wavelengths, the source, as a whole, is well represented by a circular Gaussian of angular size (FWHM) 0.35 mas. Figure 3 illustrates the suitability of DA 193 as a VLBI calibrator. While resolved, the source possesses a simple structure which is essentially circularly symmetric.

III. ANALYSIS OF OBSERVATIONS

We now proceed to find models of the source consistent with both the VLBI observations and the integrated spectrum. The analysis was identical to the analysis carried out in Paper I. The revised model is:

Component 1:

$$S_0 = 3.09 \text{ Jy}, \quad \nu_1 = 5.57 \text{ GHz}, \quad \gamma = 2;$$

Component 2:

$$S_0 = 4.88 \text{ Jy}, \quad \nu_1 = 2.73 \text{ GHz}, \quad \gamma = \frac{5}{2}.$$

As defined in Paper I, the frequency ν_1 is a fiducial frequency roughly equivalent to the frequency of flux density maximum, S_0 is a flux density scale factor, and γ is the spectral index of the (power-law) electron spectrum.

This model is shown in Figure 1b along with the VLBI component measurements taken from Table 1 and from Paper I. The solid curves represent the model fits to the compact and extended components. The sum of the component spectra is represented by the dashed curve (in both Figs. 1a and 1b) which provides an excellent fit to the total spectrum.

A similarly good fit to the total spectrum can be obtained by a single component with $S_0 = 6.86$ Jy, $\nu_1 = 3.28$ GHz, and $\gamma = 2$. This model cannot, of course, account for the structural detail of the source indicated by the VLBI observations and should be used only in describing the source as a whole.

The superior resolution of the present observations allows us to calculate a more precise estimate of the magnetic field strength. Using the revised two-component model, we calculate values of 6.7×10^{-4} and 1.6×10^{-4} G for the magnetic field strength in the compact and extended components, respectively, with about 50% uncertainty. An analysis undertaken by one of the authors (A. L. F.) indicates that virtually identical (within 20%) values are obtained if one uses a model

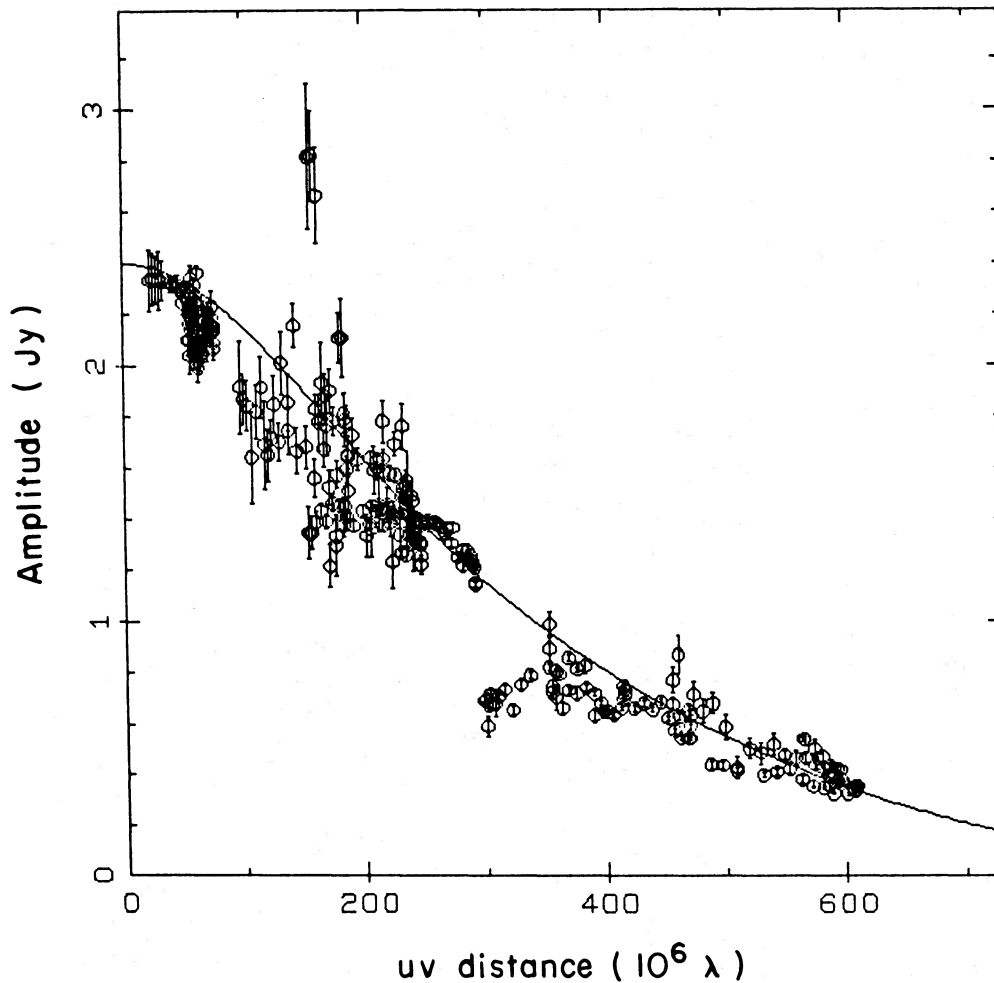


FIG. 3.—Plot of fringe amplitude vs. baseline length. The few discrepant points are assumed due to remaining calibration errors. The solid line represents the model presented in Table 1.

geometry of homogeneous spheres rather than cylinders viewed parallel to their axes.

Table 2 summarizes the results of the magnetic field estimates as follows: Column (2) lists the Gaussian-equivalent angular size (FWHM) in milli-arcsec; column (3), the normalization constant S_0 (Jy); column (4), the fiducial frequency ν_1 (GHz); column (5), the spectral index of the energetic electron spectrum; column (6), the magnetic field estimate and its estimated error; column (7), the equipartition magnetic field value; and column (8) the ratio of equipartition to “actual” magnetic field strength.

The values for the equipartition magnetic field are taken from Paper I. It was unnecessary to recalculate these values since the source has shown negligible variability during the

interval between our observations and those in Paper I. Although we find the source to be slightly more compact, the equipartition magnetic field is only weakly dependent on angular size (Miley 1980), so any corrections would be negligible compared with the uncertainties in the field strength estimates.

IV. DISCUSSION

The VLBI observations described in this paper were undertaken with the hope that higher resolution would yield an improved structural model of the source 0552+398. Better knowledge of the source structure would then allow a more precise estimate of the magnetic field strength.

Table 2 contains the main results of this paper. The

TABLE 2
MAGNETIC FIELD ESTIMATES IN 0552+398

Component (1)	θ (FWHM) (mas) (2)	S_0 (Jy) (3)	ν_1 (GHz) (4)	γ (5)	B (G) (6)	B_{eq}^a (G) (7)	R (8)
1.....	0.25	3.09 ± 0.40	5.57 ± 0.30	2	$(6.7 \pm 3.0) \times 10^{-4}$	0.26	388
2.....	0.63	4.88 ± 0.30	2.73 ± 0.10	5/2	$(1.6 \pm 0.7) \times 10^{-4}$	0.09	563

^a Values taken from Spangler *et al.* 1983.

improved estimates of the magnetic field strength confirm that the source is indeed out of equipartition in the sense that particle energy dominates magnetic field energy. We note that the magnetic field estimates are somewhat lower (about a factor of 6) than the magnetic field strength estimates given for the same components in Paper I. This is not surprising, since we find the value of the fiducial frequency, ν_1 , for the compact component to be lower than previously reported. The extended component is also more compact than indicated in the analysis of Paper I. Since the magnetic field strength is proportional to high powers of these parameters, we expect lower field estimates for both components. Nonetheless, given the large frequency range over which we have studied this source, it is the similarities, rather than the differences, in structural parameters and magnetic field estimates which are impressive. These lead us to conclude that factors such as source inhomogeneity, unaccounted for in our analysis, produce relatively minor corrections to our results.

These revised estimates exacerbate the energetics problem with this object. The ratio of the true energy density to the minimum energy density is $\sim \frac{1}{2}R^{-\delta}$, where R is the ratio of magnetic field strength to equipartition magnetic field strength, and δ is $(\gamma + 1)/2$. Using the data presented in Table 2, we conclude that "true" energy densities exceed the minimum energy values by a factor of 3000 for the more compact component, and about 30,000 for the extended component.

This extreme situation is moderated somewhat if one posits bulk relativistic motion of the radiating material. However, as noted above, the absence of pronounced variability removes any other evidence for relativistic motion.

We now briefly consider the relationship of 0552+398 to other types of compact extragalactic radio sources. Although the integrated spectrum of 0552+398 resembles that of a single, homogeneous synchrotron source, our interferometric observations indicate that the source is comprised of at least two subcomponents. These components become optically thick at different frequencies. This suggests a comparison with the compact double sources described by Phillips and Mutel (1982), which also have integrated spectra characteristic of a

fairly homogeneous, self-absorbed synchrotron source. As is the case with DA 193, the components of compact doubles usually become optically thick at different frequencies (Mutel, Hodges, and Phillips 1985). In other respects, DA 193 differs from compact doubles. Compact doubles generally tend to be unidentified, whereas DA 193 is a quasar. The separation of the components of compact doubles greatly exceeds that of the two components of 0552+398. For DA 193 to be a compact double, the source axis would have to be nearly parallel to the line of sight.

We also note that 0552+398 does not conform to the ubiquitous "core-jet" structure (Kellermann and Pauliny-Toth 1981). Such jets are almost certainly responsible for the flat or complex spectra which characterize most compact extragalactic sources. They are also the sites of superluminal motion (e.g., Walker *et al.* 1984); it may be contended that variability and other "superluminal" effects are due to relativistic beams associated with the jets. Finally, nascent VLBI polarimetric observations (Roberts *et al.* 1984) indicate that the linearly polarized flux density in compact sources originates in the jets rather than the cores.

Given these observations, we conjecture that the peaked spectrum, compact structure, relative absence of variability, and relatively low-fractional polarization of DA 193 result from its consisting of a "naked" core, without a jet. While it is true that 22 GHz is too high a frequency at which to observe jets, which tend to have relatively steep spectra, our results indicate little change in source structure between 6 and 22 GHz. Indirect arguments based on the spectrum of this source indicate that the same structure probably characterizes the source at 1 GHz. These considerations then preclude the existence of a significant jet.

The authors thank the participating observatories of the US VLBI Network. We also thank Scott Allendorf for furnishing unpublished flux density measurements. This research is supported by grants AST 82-17714 and AST 82-16890 from the National Science Foundation.

REFERENCES

- Allendorf, S. C. 1985, M.S. thesis, University of Iowa.
 Kellermann, I. K., and Pauliny-Toth, I. I. K. 1981, *Ann. Rev. Astr. Ap.*, **19**, 373.
 Miley, G. 1980, *Ann. Rev. Astr. Ap.*, **18**, 165.
 Mutel, R. L., Hodges, M., and Phillips, R. 1985, *Ap. J.*, **290**, 86.
 Owen, F. N., Spangler, S. R., and Cotton, W. D. 1980, *A.J.*, **85**, 351.
 Phillips, R. B., and Mutel, R. L. 1982, *Astr. Ap.*, **106**, 21.
 Readhead, A. C. S., and Wilkinson, P. N. 1978, *Ap. J.*, **223**, 25.
 Roberts, D. H., Potash, R. I., Wardle, J. F. C., Rogers, A. E. E., and Burke, B. F. 1984, in *IAU Symposium 110, VLBI and Compact Radio Sources*, ed. C. Fanti, K. Kellermann, and G. Setti (Dordrecht: Reidel), p. 35.
 Schilizzi, R. T., and Shaver, P. A. 1981, *Astr. Ap.*, **96**, 365.
 Spangler, S. R. 1980, *Ap. Letters*, **20**, 123.
 ———. 1982, VLA Scientific Memorandum 143, National Radio Astronomy Observatory, Charlottesville.
 Spangler, S. R., and Cotton, W. D. 1982, in *Low Frequency Variability of Extragalactic Radio Sources*, ed. W. D. Cotton and S. R. Spangler (Green Bank, W. Va.: NRAO), p. 39.
 Spangler, S. R., Mutel, R. L., and Benson, J. M. 1983, *Ap. J.*, **271**, 44 (Paper I).
 Walker, R. C., Benson, J. M., Seielstad, G. A., and Unwin, S. C. 1984, in *IAU Symposium 110, VLBI and Compact Radio Sources*, ed. C. Fanti, K. Kellermann, and G. Setti (Dordrecht: Reidel), p. 121.

JOHN M. BENSON: The National Radio Astronomy Observatory, Edgemont Road, Charlottesville, VA 22901

ALAN L. FEY, R. L. MUTEL, and STEVEN R. SPANGLER: Department of Physics and Astronomy, University of Iowa, Iowa City, IA 52242